e-ISSN 3050-9653
p-ISSN 2805-4364

10.5281/ZENODO.17621884 VOLUME 08 ISSUE 10 OCTOBER - 2025 ARTICLE ID: #02163

Numerical Methods for Addressing Fractional Order Trypanosomiasis Through the Generalized Adams-Bashforth-Moulton Approach

By Author(s):

Musa Yunusa[1,2], Omale David[1], Joseph Egbemhenghe[3], Godwin Onuche Acheneje[1,2], William Atokolo[1,2]*

[1] Department of Mathematical Sciences, Prince Abubakar Audu University, Anyigba, Nigeria

[2] Laboratory of Mathematical Epidemiology, Prince Abubakar Audu University, Anyigba

[3] Department of Mathematics Education, Prince Abubakar Audu University, Anyigba, Nigeria

Corresponding author: williamsatokolo@gmail.com

Abstract:

Trypanosomiasis remains a critical vector-borne disease burden, especially in sub-Saharan African communities where tsetse fly populations thrive and healthcare infrastructure remains limited. Conventional integer-order mathematical frameworks frequently inadequately represent the hereditary characteristics and intricate transmission patterns inherent in vector-borne disease systems. This research presents a fractional-order mathematical framework for examining the epidemiological characteristics of trypanosomiasis transmission, with particular focus on how treatment interventions at different disease stages affect overall transmission dynamics. The primary goal is to explore how variations in treatment efficacy rates and vector-human contact patterns influence disease persistence and spread within affected populations. The framework employs fractional derivatives to more accurately capture the non-Markovian properties of infection progression and immune response mechanisms. The computational results further reveal that strategically implemented treatment protocols can dramatically reduce infection prevalence, potentially driving the system toward disease elimination scenarios. The innovation of this work centers on applying fractional calculus to trypanosomiasis transmission modeling, an approach relatively unexplored in this epidemiological context, while simultaneously incorporating multi-stage treatment interventions and natural immunity waning processes. The model demonstrates superior precision in representing temporal disease progression compared to classical integer-order approaches. This investigation underscores the utility of fractional-order modeling in vector-borne disease research and emphasizes the critical importance of strengthening treatment capacity and vector control measures to effectively manage and eliminate trypanosomiasis transmission in endemic regions.

Keywords:

Trypanosomiasis, *Fractional-order analysis*, *Adam-Bashforth-Moulton*, *Numerical Simulations*.

How to cite: Yunusa, M., David, O., Egbemhenghe, J., Onuche Acheneje, G., & Atokolo, W. (2025). Numerical Methods for Addressing Fractional Order Trypanosomiasis Through the Generalized Adams-Bashforth-Moulton Approach. *GPH-International Journal of Applied Science*, 8(10), 148-171. https://doi.org/10.5281/zenodo.17621884

1.0 Introduction

Human African Trypanosomiasis (HAT), commonly known as sleeping sickness, is a vector-borne parasitic disease transmitted by tsetse flies (Glossina species) that poses a significant public health threat across sub-Saharan Africa Franco et al. (2018). The disease is caused by two subspecies of Trypanosoma brucei: T. b. gambiense, which causes chronic infection primarily in West and Central Africa, and T. b. rhodesiense, which causes acute infection in East and Southern Africa Büscher et al. (2017), Kennedy et al. (2019). HAT affects approximately 70 million people living in at-risk areas across 36 countries in sub-Saharan Africa, with an estimated 300,000 to 500,000 people currently infected W.H.O (2023). The disease progresses through two distinct stages: the hemolymphatic stage, where parasites multiply in subcutaneous tissues, blood, and lymph, and the meningo-encephalitic stage, where parasites cross the blood-brain barrier and invade the central nervous system Steverding (2008). Without proper treatment, HAT is invariably fatal, making early diagnosis and intervention critical for patient survival Malvy, and Chappuis, (2011). Despite significant progress in reducing HAT incidence through enhanced surveillance, vector control, and improved treatment protocols, the disease remains endemic in many rural communities with limited access to healthcare infrastructure Simarro et al. (2012), Pandey et al. (2015). The World Health Organization has set ambitious targets for HAT elimination as a public health problem by 2030, necessitating innovative approaches to understand transmission dynamics and optimize control strategies W.H.O (2020). Mathematical modeling serves as an essential tool for analyzing disease transmission patterns, evaluating intervention effectiveness, and guiding policy decisions in infectious disease control Heesterbeek et al. (2015), Rock et al. (2015).

Traditional mathematical models using integer-order differential equations have provided valuable insights into HAT transmission dynamics but often fail to capture the complex biological processes inherent in host-vector-parasite interactions Anderson, and May (1991). These conventional models inadequately represent the memory effects, hereditary properties, and long-term dependencies that characterize real biological systems Diethelm (2010),. Fractional-order mathematical modeling has emerged as a powerful alternative that addresses these limitations by incorporating non-local characteristics and memory effects through fractional derivatives Podlubny (1999), Kilbas (2006. Fractional differential equations (FDEs) offer enhanced modeling capabilities that extend beyond classical integer-order approaches by providing a more flexible framework for investigating complex dynamical systems Baleanu et al. (2012). These models utilize fractional derivatives, such as Caputo and Riemann-Liouville operators, which possess singular kernels and excel at capturing memory effects in biological processes Caputo and Fabrizio (2015). Additionally, non-singular kernel derivatives, including Mittag-Leffler and Atangana-Baleanu operators, have gained prominence due to their superior applicability in modeling real-world phenomena Atangana, and Baleanu (2016). Recent advances in fractional calculus applications to epidemiological modeling have demonstrated significant improvements in describing disease transmission dynamics across various infectious diseases Sun et al. (2018). For instance, Atangana and Araz (2020) developed a fractional-order model for COVID-19 transmission using Atangana-Baleanu derivatives, showing enhanced prediction accuracy compared to classical models. Similarly, Baleanu et al. (2020) applied fractional calculus to analyze HIV/AIDS dynamics, demonstrating superior model flexibility and realistic behavior representation. Khan et al. (2020), investigated malaria transmission using Caputo fractional derivatives, revealing that fractional-order models better captured the complexity of host-vector interactions and long-term epidemic trends.

The Adams-Bashforth method has proven particularly effective for solving fractional differential equations in epidemiological applications, providing stable and accurate numerical solutions Diethelm et al. (2002) Diethelm and Ford (2004), pioneered the application of fractional Adams-Bashforth-Moulton methods for solving nonlinear fractional differential equations, establishing theoretical foundations for their implementation. Pinto and Machado (2013) utilized the Adams-Bashforth method to model fractional-order dynamics in tuberculosis transmission, demonstrating improved convergence properties and computational efficiency. More recently, Ahmed and El-Sayed (2007) applied the Adams-Bashforth method to analyze hepatitis B virus dynamics using fractional calculus, showing enhanced model performance in capturing disease progression patterns. Several studies have successfully employed the Adams-Bashforth method in fractional-order disease modeling applications. Arafa et al. (2012) used this approach to investigate fractional-order HIV infection models, demonstrating superior numerical stability compared to other methods. Sweilam et al. (2007) applied the Adams-Bashforth method to solve fractional epidemic models for influenza transmission, revealing enhanced accuracy in long-term predictions. Additionally, El-Sayed et al. (2007) utilized this method to analyze fractional SIR models for measles dynamics, showing improved computational performance and solution convergence. Further research by Odibat and Shawagfeh (2007) employed the Adams-Bashforth method for solving fractional-order systems in epidemiology, emphasizing its effectiveness in handling complex nonlinear dynamics. Momani and Odibat (2007), demonstrated the method's applicability to fractional predator-prey models with epidemiological implications, while Hashim et al. (2009) applied it to fractional-order models of infectious disease outbreaks with vaccination strategies. These studies collectively highlight the Adams-Bashforth method's versatility and reliability in fractional-order epidemiological modeling. The integration of fractional calculus with the Adams-Bashforth method offers significant advantages for modeling complex biological systems like HAT transmission (2010). This approach provides enhanced computational stability, improved solution accuracy, and better representation of memory effects inherent in disease transmission processes Daftardar-Gejji, and Jafari, (2006). Furthermore, fractional-order models solved using Adams-Bashforth methods demonstrate superior performance in capturing long-term dependencies and non-local interactions that characterize vector-borne disease dynamics Garrappa, (2018). Recent applications of fractional-order modeling to vector-borne diseases have shown promising results. Mandal et al. (2021) developed a fractional model for dengue fever transmission using Caputo derivatives and Adams-Bashforth numerical methods, revealing enhanced prediction capabilities for epidemic patterns. Similarly, Kumar et al. (2017) applied fractional calculus to chikungunya virus dynamics, employing Adams-Bashforth-Moulton methods to demonstrate improved model stability and biological realism. These studies underscore the potential of fractional-order approaches in understanding and controlling vector-borne disease transmission.

The primary objectives of this study are to: (1) develop a comprehensive fractional-order mathematical model for HAT transmission incorporating both human and tsetse fly population dynamics; (2) analyze the model's mathematical properties, including existence, uniqueness, and stability of solutions; (3) implement the Adams-Bashforth method for numerical solution of the fractional differential equation system; and (4) conduct sensitivity analysis and numerical simulations to evaluate the effectiveness of various control strategies.

This research addresses a significant gap in the literature by combining fractional calculus with the Adams-Bashforth method to model HAT transmission dynamics comprehensively. The study contributes to the growing body of knowledge on fractional-order epidemiological

modeling while providing practical insights for HAT control and elimination strategies. The manuscript is organized as follows: Section 2 presents the fractional-order model formulation, Section 3 analyzes mathematical properties and stability, Section 4 discusses numerical methods and simulation results, and Section 5 provides conclusions and recommendations for future research.

Definition 1:

Let $f \in \Lambda^{\infty}(R),$ then the left and right Caputo fractional derivative of the function f is given by

$$ {}^{c}D_{t}^{\gamma} f(t) = \left(t^{0}D_{t}^{-(m-\gamma)} \left(\frac{d}{dt} \right)^{m} f(t) \right)$$

$$ {}^{c}D_{t}^{\gamma} f(t) = \frac{1}{\Gamma(m-\gamma)} \int_{0}^{t} \left((t-\lambda)^{m-\gamma-1} f^{m}(\lambda) \right) d\lambda \qquad (1)$$

The same way

$$ {}_{T}^{c}D_{t}^{\gamma} f(t) = \left({}_{t}D_{T}^{-(m-\gamma)} \left(\frac{-d}{dt} \right)^{m} f(t) \right)$$

$$ {}_{T}^{c}D_{T}^{\gamma} f(t) = \frac{(-1)^{m}}{\Gamma(m-\gamma)} \int_{t}^{T} \left((\lambda-t)^{m-\gamma-1} f^{m}(\lambda) \right) d\lambda$$

Definition 2: The generalized Mittag-Leffler function $E_{\alpha,\beta}(x)$ for $x \in R$ is given by

$$ E_{\alpha,\beta}(x) = \sum_{m=0}^{\infty} \frac{x^{m}}{\Gamma(\alpha m + \beta)}, \alpha, \beta > 0 \qquad (2)$$

which can also be represented as

$$ E_{\alpha,\beta}(x) = xE_{\alpha,\alpha+\beta(x)} + \frac{1}{\Gamma(\beta)} \qquad (3)$$

$$ E_{\alpha,\beta}(x) = L\left[t^{\beta-1} E_{\alpha,\beta}\left(\pm \psi t^{\alpha} \right) \right] = \frac{S^{\alpha-\beta}}{S^{\alpha} \pm \psi} \qquad (4)$$

Proposition 1.1.

Let $f \in \Lambda^{\infty}(R) \cap C(R)$ and $\alpha \in R, m-1 < \alpha < m,$

Therefore, the conditions given below holds:

1. ${}_{t_0}^{c}D_{t}^{\gamma} I^{\gamma} f(t) = f(t)$

2. $I_{t_0}^{\gamma} D_t^{\gamma} f(t) = f(t) - \sum_{k=0}^{m-k} \frac{t^k}{k!} f^k(t_o)$.

2.0 Model Formulation

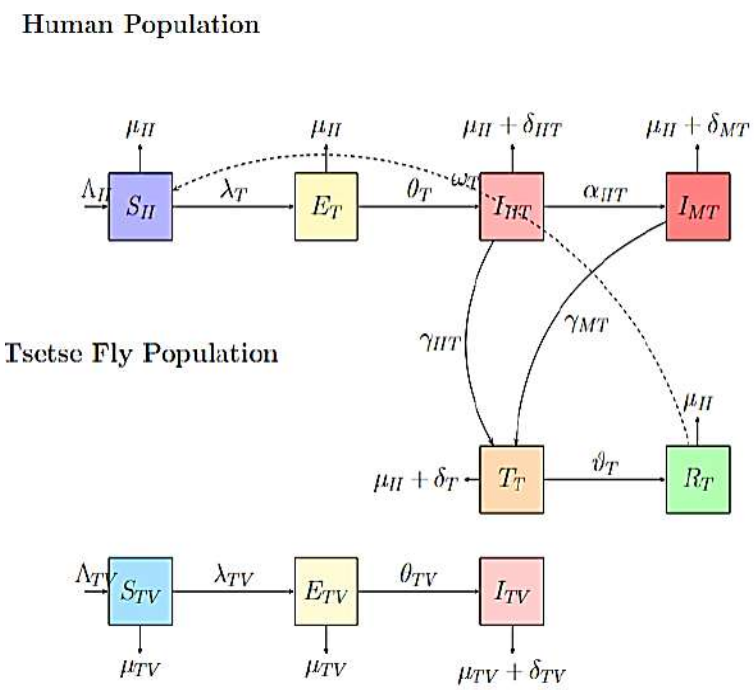

Figure 2: Schematic Diagram of the trypanosomiasis model

2.1 Model Description

The rate at which individuals enter the susceptible human population is represented as Λ_H so that β_T represents the effective contact rate between susceptible individuals and infected tsetse flies. We denote ω_T represents the rate of re-susceptibility of recovered humans from trypanosomiasis, θ_T is the progression rate from E_T compartment to I_{HT} compartment. α_{HT} is the progression rate from I_{HT} compartment to I_{MT} compartment. β_{TV} transmission probability of trypanosomiasis from infected humans to susceptible tsetse flies. The natural death rate of humans is denoted as μ_H . Humans die due to the infectiousness of hemolymphatic trypanosomiasis at the rate δ_{HT} . The parameter γ_{HT} represents the treatment rate for humans infected with hemolymphatic trypanosomiasis, while γ_{MT} denotes the treatment rate for humans infected with meningo-encephalitic trypanosomiasis. The recovery rate from trypanosomiasis treatment is represented by ϑ_T , which transitions individuals from the treatment compartment T_T to the recovered compartment R_T . Disease-induced mortality occurs at different stages, with δ_{MT} representing the death rate for meningo-encephalitic trypanosomiasis and δ_T representing the death rate for individuals in the treatment class. For the tsetse fly population dynamics, Λ_{TV} represents the recruitment rate of susceptible tsetse flies into the vector population. The natural mortality rate of tsetse flies is denoted as μ_{TV}, while δ_{TV} represents the disease-induced death rate for infected tsetse flies. The parameter

θ_{TV} describes the progression rate from exposed tsetse flies (E_{TV}) to infected tsetse flies (I_{TV}). The biting rate of tsetse flies, which determines the frequency of contact between vectors and humans, is represented by m_T .

The force of infection parameters play crucial roles in disease transmission dynamics. For human infection, $\lambda_T = \frac{m_T \beta_T I_{TV}}{N_H}$ represents the per capita rate at which susceptible humans acquire trypanosomiasis infection from infected tsetse flies. Conversely, for vector infection, $\lambda_{TV} = \frac{m_T \beta_{TV} (I_{HT} + I_{MT} + T_T)}{N_H}$ represents the per capita rate at which susceptible tsetse flies become infected through contact with infected humans in various disease stages. The total human population N_H serves as the normalization factor, ensuring that the force of infection appropriately scales with population density.

2.2 Model Equations

The differential equations for the trypanosomiasis transmission dynamics in the human and vector population are:

$$\frac{dS_H}{dt} = \Lambda_H - \lambda_T S_H - \mu_H S_H + \omega_T R_T$$

$$\frac{dE_T}{dt} = \lambda_T S_H - (\theta_T + \mu_H) E_T$$

$$\frac{dI_{HT}}{dt} = \theta_T E_T - (\alpha_{HT} + \gamma_{HT} + \delta_{HT} + \mu_H) I_{HT}$$

$$\frac{dI_{MT}}{dt} = \alpha_{HT} I_{HT} - (\gamma_{MT} + \delta_{MT} + \mu_H) I_{MT}$$

$$\frac{dT_T}{dt} = \gamma_{HT} I_{HT} + \gamma_{MT} I_{MT} - (\vartheta_T + \delta_T + \mu_H) T_T \qquad (5)$$

$$\frac{dR_T}{dt} = \vartheta_T T_T - (\omega_T + \mu_H) R_T$$

$$\frac{dS_{TV}}{dt} = \Lambda_{TV} - (\lambda_{TV} + \mu_{TV}) S_{TV}$$

$$\frac{dE_{TV}}{dt} = \lambda_{TV} S_{TV} - (\theta_{TV} + \mu_{TV}) E_{TV}$$

$$\frac{dI_{TV}}{dt} = \theta_{TV} E_{TV} - (\delta_{TV} + \mu_{TV}) I_{TV}$$

The force of infection for trypanosomiasis in the human population:

$$\lambda_T = \frac{m_T \beta_T I_{TV}}{N_H}$$

The force of infection for trypanosomiasis in the tsetse fly population:

$$\lambda_{TV} = \frac{m_T \beta_{TV} (I_{HT} + I_{MT} + T_T)}{N_H}$$

where $N_H = S_H + E_T + I_{HT} + I_{MT} + T_T + R_T$ is the total human population.

3.0 Fractional Trypanosomiasis mathematical model

In this section, we extend the integer-order trypanosomiasis model from the differential equations by incorporating the Caputo fractional derivative operator. This modified model offers greater flexibility compared to the classical model, as the fractional-order formulation allows for varying outputs and diverse response behaviors. The fractional trypanosomiasis model is thus presented as follows:

$$\begin{aligned}
{}^{C}D_t^{\gamma} S_H &= \Lambda_H - \lambda_T S_H - \mu_H S_H + \omega_T R_T \\
{}^{C}D_t^{\gamma} E_T &= \lambda_T S_H - (\theta_T + \mu_H) E_T \\
{}^{C}D_t^{\gamma} I_{HT} &= \theta_T E_T - (\alpha_{HT} + \gamma_{HT} + \delta_{HT} + \mu_H) I_{HT} \\
{}^{C}D_t^{\gamma} I_{MT} &= \alpha_{HT} I_{HT} - (\gamma_{MT} + \delta_{MT} + \mu_H) I_{MT} \\
{}^{C}D_t^{\gamma} T_T &= \gamma_{HT} I_{HT} + \gamma_{MT} I_{MT} - (\vartheta_T + \delta_T + \mu_H) T_T \qquad (6) \\
{}^{C}D_t^{\gamma} R_T &= \vartheta_T T_T - (\omega_T + \mu_H) R_T \\
{}^{C}D_t^{\gamma} S_{TV} &= \Lambda_{TV} - (\lambda_{TV} + \mu_{TV}) S_{TV} \\
{}^{C}D_t^{\gamma} E_{TV} &= \lambda_{TV} S_{TV} - (\theta_{TV} + \mu_{TV}) E_{TV} \\
{}^{C}D_t^{\gamma} I_{TV} &= \theta_{TV} E_{TV} - (\delta_{TV} + \mu_{TV}) I_{TV}
\end{aligned}$$

Subject to positive initial conditions

$$\begin{aligned}
&S_H(0) = S_{H0}, E_T(0) = E_{T0}, I_{HT}(0) = I_{HT0}, I_{MT}(0) = I_{MT0}, T_T(0) = T_{T0}, \\
&R_T(0) = R_{T0}, S_{TV}(0) = S_{TV0}, E_{TV}(0) = E_{TV0}, I_{TV}(0) = I_{TV0}.
\end{aligned}$$

3.1 Positivity of model solution

We considered the non-negativity of the initial values $N(t) \le \frac{\Lambda_H}{\mu_H}$ as $t \to \infty$

Secondly, if $, \limsup N_0(t) \le \frac{\pi}{\mu},$

then our model feasible domain is given by:

$$\Omega = \left\{ \begin{array}{l} \left(S_H, E_T, I_{HT}, I_{MT}, T_T, R_T, S_{TV}, E_{TV}, I_{TV}\right) \subset R+^9 : \\ S_H + E_T + I_{HT} + I_{MT} + T_T + R_T + S_{TV} + E_{TV} + I_{TV} \le \frac{\Lambda_H}{\mu_H} \end{array} \right\}$$

so that $\Omega = \Omega_H \subset R+^9,$

hence, Ω is positively invariant.

If $S_{H0}, E_{T0}, I_{HT0}, I_{MT0}, T_{T0}, R_{T0}, S_{TV0}, E_{TV0}, I_{TV0}$ are non-negative, then the solution of model (6) will be non-negative for $t > 0$. From Eq. (6), picking the first equation, we have that

$$^C D_t^\gamma S_H = \Lambda_H - \lambda_T S_H - \mu_H S_H + \omega_T R_T$$

$$^C D_t^\gamma S_H = \Lambda_H - (\lambda_T + \mu_H) S_H + \omega_T R_T$$

$$^C D_t^\gamma S_H + (\lambda_T + \mu_H) S_H - \omega_T R_T = \Lambda_H$$

But $\Lambda_H \ge 0$ then $^C D_t^\gamma S_H + (\lambda_T + \mu_H) S_H - \omega_T R_T \ge 0$

Applying the Laplace transform we obtained: $L\left[{}^C D_t^\gamma S_H \right] + L\left[(\lambda_T + \mu_H) S_H \right] \ge 0$

$$s^\gamma SH(s) - s^{\gamma-1} SH(0) + (\lambda_T + \mu_H) S_H(s) \ge 0$$

$$SH(s) \ge \frac{s^{\gamma-1}}{s^\gamma + (\lambda T + \mu_H)} S_H(0)$$

By taking the inverse Laplace transform, we obtained:

$$S_H(t) \ge E_{\gamma,1}\left(-(\lambda_T + \mu_H) t^\gamma\right) S_{H0} \qquad (7)$$

Now since the term on the right hand side of Eq. (7) is positive, we conclude that $S_H \ge 0$ *for* $t \ge 0$. In the same way, we also have that

$$E_T \geq 0, I_{HT} \geq 0, I_{MT} \geq 0, T_T \geq 0, R_T \geq 0, S_{TV} \geq 0, E_{TV} \geq 0, I_{TV} \geq 0$$

that is are positives, therefore, the solution will remain in $R+^9$ for all $t \geq 0$ with positive initial conditions.

3.2 Existence and uniqueness of our model solution

Let the real non-negative be J, we consider $L = [0, K]$.

The set of all continuous functions that is defined on M is represented by $N_e^0(L)$ with norm as;

$|X| = \sup\{|K(t)|, t \in L\}$. Considering model (6) with initial conditions presented in (8) which can be denoted as an initial value problem (IVP) in (13).

$$^c D_t^\gamma (t) = Z(t, X(t)), \quad 0 < t < J < \infty, \; X(0) = X_0.$$

Where

$Y(t) = (S_H(t), E_T(t), I_{HT}(t), I_{MT}(t), T_T(t), R_T(t), S_{TV}(t), E_{TV}(t), I_{TV}(t))$ represents the classes and Z is a continuous function defined as follows;

$$Z(t, X(t)) = \begin{pmatrix} Z_1(t, S_H(t)) \\ Z_2(t, E_T(t)) \\ Z_3(t, I_{HT}(t)) \\ Z_4(t, I_{MT}(t)) \\ Z_5(t, T_T(t)) \\ Z_6(t, R_T(t)) \\ Z_7(t, S_{TV}(t)) \\ Z_8(t, E_{TV}(t)) \\ Z_9(t, I_{TV}(t)) \end{pmatrix} = \begin{pmatrix} \Lambda_H - \lambda_T S_H - \mu_H S_H + \omega_T R_T \\ \lambda_T S_H - (\theta_T + \mu_H) E_T \\ \theta_T E_T - (\alpha_{HT} + \gamma_{HT} + \delta_{HT} + \mu_H) I_{HT} \\ \alpha_{HT} I_{HT} - (\gamma_{MT} + \delta_{MT} + \mu_H) I_{MT} \\ \gamma_{HT} I_{HT} + \gamma_{MT} I_{MT} - (\vartheta_T + \delta_T + \mu_H) T_T \\ \vartheta_T T_T - (\omega_T + \mu) R_T \\ \Lambda_{TV} - \left(\frac{m_T \beta_{TV} (I_{HT} + I_{MT} + T_T)}{N_H} + \mu_{TV} \right) S_{TV} \\ \frac{m_T \beta_{TV} (I_{HT} + I_{MT} + T_T)}{N_H} - (\theta_{TV} + \mu_{TV}) E_{TV} \\ \theta_{TV} E_{TV} - (\delta_{TV} + \mu_{TV}) I_{TV} \end{pmatrix}, \tag{8}$$

Using proposition (2.1), we have that,

$$S_H(t) = S_{H0} + I_t^\gamma [\Lambda_H - \lambda_T S_H - \mu_H S_H + \omega_T R_T],$$

$$E_T(t) = E_{T0} + I_t^\gamma [\lambda_T S_H - (\theta_T + \mu_H) E_T], \tag{9}$$

$$I_{HT}(t) = I_{HT0} + I_t^{\gamma}\left[\theta_T E_T - (\alpha_{HT} + \gamma_{HT} + \delta_{HT} + \mu_H) I_{HT}\right],$$
$$I_{MT}(t) = I_{MT0} + I_t^{\gamma}\left[\alpha_{HT} I_{HT} - (\gamma_{MT} + \delta_{MT} + \mu_H) I_{MT}\right],$$

$$T_T(t) = T_{T0} + I_t^{\gamma}\left[\gamma_{HT} I_{HT} + \gamma_{MT} I_{MT} - (\vartheta_T + \delta_T + \mu_H) T_T\right],$$

$$R_T(t) = R_{T0} + I_t^{\gamma}\left[\vartheta_T T_T - (\omega_T + \mu) R_T\right],$$

$$S_{TV}(t) = S_{TV0} + I_t^{\gamma}\left[\Lambda_{TV} - \frac{m_T \beta_{TV}(I_{HT} + I_{MT} + T_T)}{N} - \mu\right] S_{TV}.$$
$$E_{TV}(t) = E_{TV0} + I_t^{\gamma}\left[\frac{m_T \beta_{TV}(I_{HT} + I_{MT} + T_T)}{N} + \mu\right] S_{TV} - (\theta_{TV} + \mu) E_{TV}$$

$$I_{TV}(t) = I_{TV0} + I_t^{\gamma}\left[\theta_{TV} E_{TV} - \mu_{TV} I_{TV}\right]$$

We obtain the Picard iteration of (9) as follows;

$$S_{Hn}(t) = S_{H0} + \frac{1}{\Gamma(\gamma)}\int_0^t (t - \lambda_T)^{\gamma-1} Z_1\left(\lambda_T, S_{Hn-1}(\lambda_T)\right) d\lambda_T,$$

$$E_{Tn}(t) = E_{T0} + \frac{1}{\Gamma(\gamma)}\int_0^t (t - \lambda_T)^{\gamma-1} Z_2\left(\lambda_T, E_{T(n-1)}(\lambda_T)\right) d\lambda_T,$$
$$I_{HTn}(t) = I_{HT0} + \frac{1}{\Gamma(\gamma)}\int_0^t (t - \lambda_T)^{\gamma-1} Z_3\left(\lambda_T, I_{HT(n-1)}(\lambda_T)\right) d\lambda_T,$$

$$I_{MTn}(t) = I_{MT0} + \frac{1}{\Gamma(\gamma)}\int_0^t (t - \lambda_T)^{\gamma-1} Z_4\left(\lambda_T, I_{MT(n-1)}(\lambda_T)\right) d\lambda_T,$$
$$T_{Tn}(t) = T_{T0} + \frac{1}{\Gamma(\gamma)}\int_0^t (t - \lambda_T)^{\gamma-1} Z_5\left(\lambda_T, T_{T(n-1)}(\lambda_T)\right) d\lambda_T,$$

$$R_{Tn}(t) = R_{T0} + \frac{1}{\Gamma(\gamma)}\int_0^t (t - \lambda_T)^{\gamma-1} Z_6\left(\lambda_T, R_{T(n-1)}(\lambda_T)\right) d\lambda_T,$$
$$S_{TVn}(t) = S_{TV0} + \frac{1}{\Gamma(\gamma)}\int_0^t (t - \lambda_T)^{\gamma-1} Z_7\left(\lambda_T, S_{TV(n-1)}(\lambda_T)\right) d\lambda_T, \quad (10)$$

$$E_{TVn}(t) = E_{TV0} + \frac{1}{\Gamma(\gamma)}\int_0^t (t - \lambda_T)^{\gamma-1} Z_8\left(\lambda_T, E_{TV(n-1)}(\lambda_T)\right) d\lambda_T,$$
$$I_{TVn}(t) = I_{TV0} + \frac{1}{\Gamma(\gamma)}\int_0^t (t - \lambda_T)^{\gamma-1} Z_9\left(\lambda_T, I_{TV(n-1)}(\lambda_T)\right) d\lambda_T.$$

Lemma 1. The Lipschitz condition described from Eq. (10) is satisfied by vector $Z\left(t, X(t)\right)$ on a set $[0, L] \times R_+^9$ with the Lipschitz constant given as;

$$\psi = \max\begin{pmatrix}(\beta_T+\mu),(\theta_T+\mu_H),(\alpha_{HT}+\gamma_{HT}+\delta_{HT}+\mu_H),(\gamma_{MT}+\delta_{MT}+\mu_H),(\vartheta_T+\delta_T+\mu_H),\\(\omega_T+\mu_H),(\lambda_{TV}+\mu_{TV}),(\theta_{TV}+\mu_{TV}),\mu_{TV}\end{pmatrix}$$

Proof.

$$\left|Z_1(t,S_H)-Z_1(t,S_{H1})\right| = \left|\Lambda_H-\lambda_T S_H-\mu_H S_H+\omega_T R_T\right|$$
$$\left|-\lambda_T S_H-\mu_H S_H(S_H-S_{H1})+\mu_H(S_H-S_{H1})\right| \le \beta_T^*\left|S_H-S_{H1}\right|+\mu_H\left|S_H-S_{H1}\right|$$

$$\therefore \left|Z_1(t,S_H)-Z_1(t,S_{H1})\right| \le (\beta_T^*+\mu)\left|S_H-S_{H1}\right|$$

Similarly, we obtained the following;

$$\left|Z_2(t,E_T)-Z_2(t,E_{T1})\right| \le (\theta_T+\mu_H)\left|E_T-E_{T1}\right|,$$
$$\left|Z_3(t,I_{HT})-Z_3(t,I_{HT1})\right| \le (\alpha_{HT}+\gamma_{HT}+\delta_{HT}+\mu_H)\left|I_{HT}-I_{HT1}\right|,$$

$$\left|Z_4(t,I_{MT})-Z_4(t,I_{MT1})\right| \le (\gamma_{MT}+\delta_{MT}+\mu_H)\left|I_{MT}-I_{MT1}\right|$$
$$\left|Z_5(t,T_T)-Z_5(t,T_{T1})\right| \le (\vartheta_T+\delta_T+\mu_H)\left|T_T-T_{T1}\right|$$

$$\left|Z_6(t,R_T)-Z_6(t,R_{T1})\right| \le (\omega_T+\mu_H)\left|R_T-R_{T1}\right|$$
$$\left|Z_7(t,S_{TV})-Z_7(t,S_{TV1})\right| \le \left(\frac{m_T\beta_{TV}(I_{HT}+I_{MT}+T_T)}{N_H}+\mu_{TV}\right)\left|S_{TV}-S_{TV1}\right|, \quad (11)$$

$$\left|Z_8(t,E_{TV})-Z_8(t,E_{TV1})\right| \le (\theta_{TV}+\mu_{TV})\left|E_{TV}-E_{TV1}\right|.$$
$$\left|Z_9(t,I_{TV})-Z_9(t,I_{TV1})\right| \le \mu_{TV}\left|I_{TV}-I_{TV1}\right|.$$

Where we obtained

$$\left|Z(t,X_1(t))-Z(t,X_2(t))\right| \le \psi\left|X_1-X_2\right|,$$

$$\psi = \max\begin{pmatrix}(\beta_T+\mu),(\theta_T+\mu_H),(\alpha_{HT}+\gamma_{HT}+\delta_{HT}+\mu_H),(\gamma_{MT}+\delta_{MT}+\mu_H),(\vartheta_T+\delta_T+\mu_H),\\(\omega_T+\mu_H),(\lambda_{TV}+\mu_{TV}),(\theta_{TV}+\mu_{TV}),\mu_{TV}\end{pmatrix}$$

3.3 The basic reproduction number (R_0^T) and model equilibrium points:

The disease-free equilibrium points of the trypanosomiasis model is expressed as:

$$(\text{HDFEP}) = \left(\left(S_H^*,E_T^*,I_{HT}^*,I_{MT}^*,T_T^*,R_T^*,S_{TV}^*,E_{TV}^*,I_{TV}^*\right) = \left(\frac{\Lambda_H}{\mu_H},0,0,0,0,0,\frac{\Lambda_{TV}}{\mu_{TV}},0,0\right)\right) \quad (12)$$

Let $n=\left(E_T, I_{HT}, I_{MT}, T_T, E_{TV}, I_{TV}\right)$

So that $\frac{dn}{dt}=F-V.$

$$F_{0T}=\begin{bmatrix} 0 & 0 & 0 & 0 & 0 & \beta_T \\ 0 & 0 & 0 & 0 & 0 & 0 \\ 0 & 0 & 0 & 0 & 0 & 0 \\ 0 & 0 & 0 & 0 & 0 & 0 \\ 0 & \frac{m\beta_{TV}\Lambda_{TV}\mu_H}{\Lambda_H\mu_{TV}} & \frac{m\beta_{TV}\Lambda_{TV}\mu_H}{\Lambda_H\mu_{TV}} & \frac{m\beta_{TV}\Lambda_{TV}\mu_H}{\Lambda_H\mu_{TV}} & 0 & 0 \\ 0 & 0 & 0 & 0 & 0 & 0 \end{bmatrix}$$

$$V_{0T}=\begin{bmatrix} K_{1T} & 0 & 0 & 0 & 0 & 0 \\ -\theta_T & K_{2T} & 0 & 0 & 0 & 0 \\ 0 & -\alpha_{HT} & K_{3T} & 0 & 0 & 0 \\ 0 & -\gamma_{HT} & -\gamma_{MT} & K_{4T} & 0 & 0 \\ 0 & 0 & 0 & 0 & K_{5T} & 0 \\ 0 & 0 & 0 & 0 & -\theta_{TV} & K_{6T} \end{bmatrix}$$

Where $K_{1T}=\left(\theta_T+\mu_H\right)$ $K_{2T}=\left(\alpha_{HT}+\gamma_{HT}+\delta_{HT}+\mu_H\right)$ $K_{3T}=\left(\gamma_{MT}+\delta_{MT}+\mu_H\right)$

$K_{4T}=\left(\vartheta_T+\delta_T+\mu_H\right)$ $K_{5T}=\left(\theta_{TV}+\mu_{TV}\right)$ $K_{6T}=\left(\delta_{TV}+\mu_{TV}\right)$

Mathematically, the basic reproduction number is computed as $R_0=\rho\left(FV^{-1}\right)$ where ρ is the dominant Eigen value of the system $\left(FV^{-1}\right)$. Where R_0^T is the basic reproduction number associated with the individuals in the population.

$$R_0=\sqrt{\frac{\beta_T\cdot m\cdot\beta_{TV}\cdot\Lambda_{TV}\cdot\mu_H}{\Lambda_H\cdot\mu_{TV}\cdot K_{5T}\cdot K_{6T}}}$$

4.0 Fractional order model numerical results

The fractional-order trypanosomiasis model was numerically solved using the generalized fractional Adams–Bashforth–Moulton method as described in Diethelm and Ford, (2004), Pinto,and Machado, J.A.T. (2013), The parameter values utilized in the model are provided in Table 1, with varying fractional-order values. (γ) are considered and simulated.

4.1. Implementation of fractional Adams–Bashforth–Moulton method

The approach outlined in Ahmed, and El-Sayed (2007), Arafa et al. (2012) is applied in this study. An approximate solution for the fractional trypanosomiasis model is obtained using the fractional Adams–Bashforth–Moulton method. The fractional trypanosomiasis model is now expressed as follows:

$$
\begin{aligned}
&{}^{c}D_{t}^{\gamma}P(t) = Q\left(t, q(t)\right), 0 < t < \beta, \qquad (13)\\
&P^{(n)}(0) = P_{0}^{(n)},,,, n = 1,0,,,..., q, q = [\gamma].
\end{aligned}
$$

Where $P = \left(S_H^*, E_T^*, I_{HT}^*, I_{MT}^*, T_T^*, R_T^*, S_{TV}^*, E_{TV}^*, I_{TV}^*\right) \in R_+^9$ and $Q\left(t, q(t)\right)$ is a real valued function that is continuous.

Eq. (13) can be therefore be represented using the concept of fractional integral as follows:

$$
P(t) = \sum_{n=0}^{m-1} P_0^{(n)} \frac{t^n}{n!} + \frac{1}{\Gamma(\gamma)} \int_0^t (t-y)^{\gamma-1} Q\left(y, q(y)\right) dy, \qquad (14)
$$

Using the method described in [24], we let the step size $g = \frac{\beta}{N},,, N \in$ with a grid that is uniform on $[0, \beta]$. Therefore, the fractional order trypanosomiasis model can be approximated as:

$$
\begin{aligned}
S_{Hk+1}(t) &= S_{H0} + \frac{g^{\gamma}}{\Gamma(\gamma+2)}\left[\Lambda_H - \frac{m_T \beta_T I_{TV}^n S_H^n}{N_H^n} - \mu_H S_H^n + \omega_T R_T^n\right]\\
&+ \frac{g^{\gamma}}{\Gamma(\gamma+2)} \sum_{y=0}^{k} d_{y,k+1}\left[\Lambda_H - \frac{m_T \beta_T I_{TVy} S_{Hy}}{N_{Hy}} - \mu_H S_{Hy} + \omega_T R_{Ty}\right]\\
E_{Tk+1}(t) &= E_{T0} + \frac{g^{\gamma}}{\Gamma(\gamma+2)}\left[\frac{m_T \beta_T I_{TV}^n S_H^n}{N_H^n} - K_{1T} E_T^n\right]\\
&+ \frac{g^{\gamma}}{\Gamma(\gamma+2)} \sum_{y=0}^{k} d_{y,k+1}\left[\frac{m_T \beta_T I_{TVy} S_{Hy}}{N_{Hy}} - K_{1T} E_{Ty}\right],\\
I_{HTk+1}(t) &= I_{HT0} + \frac{g^{\gamma}}{\Gamma(\gamma+2)}\left[\theta_T E_T^n - K_{2T} I_{HT}^n\right]\\
&+ \frac{g^{\gamma}}{\Gamma(\gamma+2)} \sum_{y=0}^{k} d_{y,k+1}\left[\theta_T E_{Ty} - K_{2T} I_{HTy}\right],\\
I_{MTk+1}(t) &= I_{MT0} + \frac{g^{\gamma}}{\Gamma(\gamma+2)}\left[\alpha_{HT} I_{HT}^n - K_{3T} I_{MT}^n\right]\\
&+ \frac{g^{\gamma}}{\Gamma(\gamma+2)} \sum_{y=0}^{k} d_{y,k+1}\left[\alpha_{HT} I_{HTy} - K_{3T} I_{MTy}\right],\\
T_{Tk+1}(t) &= T_{T0} + \frac{g^{\gamma}}{\Gamma(\gamma+2)}\left[\gamma_{HT} I_{HT}^n + \gamma_{MT} I_{MT}^n - K_{4T} T_T^n\right]\\
&+ \frac{g^{\gamma}}{\Gamma(\gamma+2)} \sum_{y=0}^{k} d_{y,k+1}\left[\gamma_{HT} I_{HTy} + \gamma_{MT} I_{MTy} - K_{4T} T_{Ty}\right],
\end{aligned}
$$

$$
\begin{aligned}
R_{Tk+1}(t) &= R_{T0} + \frac{g^{\gamma}}{\Gamma(\gamma+2)}\left[\vartheta_T T_T^n - (\omega_T + \mu_H)R_T^n\right] \\
&+ \frac{g^{\gamma}}{\Gamma(\gamma+2)}\sum_{y=0}^{k} d_{y,k+1}\left[\vartheta_T T_{Ty} - (\omega_T + \mu_H)R_{Ty}\right], \\
S_{TVk+1}(t) &= S_{TV0} + \frac{g^{\gamma}}{\Gamma(\gamma+2)}\left[\Lambda_{TV} - \frac{m_T\beta_{TV}(I_{HT}^n + I_{MT}^n + T_T^n)S_{TV}^n}{N_H^n} - \mu_{TV}S_{TV}^n\right] \\
&+ \frac{g^{\gamma}}{\Gamma(\gamma+2)}\sum_{y=0}^{k} d_{y,k+1}\left[\Lambda_{TV} - \frac{m_T\beta_{TV}(I_{HTy} + I_{MTy} + T_{Ty})S_{TVy}}{N_{Hy}} - \mu_{TV}S_{TVy}\right], \\
E_{TVk+1}(t) &= E_{TV0} + \frac{g^{\gamma}}{\Gamma(\gamma+2)}\left[\frac{m_T\beta_{TV}(I_{HT}^n + I_{MT}^n + T_T^n)S_{TV}^n}{N_H^n} - K_{5T}E_{TV}^n\right] \\
&+ \frac{g^{\gamma}}{\Gamma(\gamma+2)}\sum_{y=0}^{k} d_{y,k+1}\left[\frac{m_T\beta_{TV}(I_{HTy} + I_{MTy} + T_{Ty})S_{TVy}}{N_{Hy}} - K_{5T}E_{TVy}\right], \\
I_{TVk+1}(t) &= I_{TV0} + \frac{g^{\gamma}}{\Gamma(\gamma+2)}\left[\theta_{TV}E_{TV}^n - K_{6T}I_{TV}^n\right] \\
&+ \frac{g^{\gamma}}{\Gamma(\gamma+2)}\sum_{y=0}^{k} d_{y,k+1}\left[\theta_{TV}E_{TVy} - K_{6T}I_{TVy}\right],
\end{aligned}
\tag{15}
$$

. Where

$$
\begin{aligned}
S_{k+1}^n(t) &= S_0 + \frac{1}{\Gamma(\gamma)}\sum_{y=0}^{k} f_{y,k+1}\left[\Lambda_H - \frac{m_T\beta_T I_{TVy}S_{Hy}}{N_{Hy}} - \mu_H S_{Hy} + \omega_T R_{Ty}\right], \\
E_{Tk+1}^n(t) &= E_{T0} + \frac{1}{\Gamma(\gamma)}\sum_{y=0}^{k} f_{y,k+1}\left[\frac{m_T\beta_T I_{TVy}S_{Hy}}{N_{Hy}} - K_{1T}E_{Ty}\right], \\
I_{HTk+1}^n(t) &= I_{HT0} + \frac{1}{\Gamma(\gamma)}\sum_{y=0}^{k} f_{y,k+1}\left[\theta_T E_{Ty} - K_{2T}I_{HTy}\right], \\
I_{MTk+1}^n(t) &= I_{MT0} + \frac{1}{\Gamma(\gamma)}\sum_{y=0}^{k} f_{y,k+1}\left[\alpha_{HT}E_{HTy} - K_{3T}I_{MTy}\right], \\
T_{Tk+1}^n(t) &= T_{T0} + \frac{1}{\Gamma(\gamma)}\sum_{y=0}^{k} f_{y,k+1}\left[\gamma_{HT}I_{HTy} + \gamma_{MT}I_{MTy} - K_{4T}T_{Ty}\right], \\
R_{Tk+1}^n(t) &= R_{T0} + \frac{1}{\Gamma(\gamma)}\sum_{y=0}^{k} f_{y,k+1}\left[\vartheta_T T_{Ty} - (\omega_T + \mu_H)R_{Ty}\right], \\
S_{TVk+1}^n(t) &= S_{TV0} + \frac{1}{\Gamma(\gamma)}\sum_{y=0}^{k} f_{y,k+1}\left[\Lambda_{TV} - \frac{m_T\beta_{TV}(I_{HTy} + I_{MTy} + T_{Ty})S_{TVy}}{N_{Hy}} - \mu_{TV}S_{TVy}\right], \\
E_{TVk+1}^n(t) &= E_{TV0} + \frac{1}{\Gamma(\gamma)}\sum_{y=0}^{k} f_{y,k+1}\left[\frac{m_T\beta_{TV}(I_{HTy} + I_{MTy} + T_{Ty})S_{TVy}}{N_{Hy}} - K_{5T}E_{TVy}\right], \\
I_{TVk+1}^n(t) &= I_{TV0} + \frac{1}{\Gamma(\gamma)}\sum_{y=0}^{k} f_{y,k+1}\left[\theta_{TV}E_{TVy} - K_{6T}I_{TVy}\right],
\end{aligned}
\tag{16}
$$

From (15) and (16) obtained:

$$d_{y,K+1} = K^{\gamma+1} - (k-\gamma)(k+\gamma)^{\gamma},,, y = 0$$

$$(k-y+2)^{\gamma+1} + (k-\gamma)^{\gamma+1} - 2(k-y+1)^{\{\gamma+1\}},1 \le y \le k$$

$$1, y = k+1$$

and

$$f_{y,k+1} = \frac{g^{\gamma}}{\gamma}\left[(k-y+1)^{\gamma} - (k-y)^{\gamma}\right],,,0 \le y \le k.$$

Table 1: Parameter Values and Sources

Parameter	Description	Value	Units	Source
Λ_H	Recruitment rate of humans	0.02	day^{-1}	Gervas et al. (2018)
Λ_{TV}	Recruitment rate of tsetse flies	0.05	day^{-1}	Rock et al. (2019)
m_T	Biting rate of tsetse flies	0.33	day^{-1}	Lord et al. (2018)
β_T	Contact rate between susceptible humans and infected tsetse flies	0.2	dimensionless	Funk et al. (2013)
β_{TV}	Contact rate between susceptible tsetse flies and infected humans	0.15	dimensionless	Hargrove et al. (2012)
ω_T	Rate of re-susceptibility of recovered humans from trypanosomiasis	0.005	day^{-1}	Checchi et al. (2018)
μ_H	Natural death rate of humans	0.000045	day^{-1}	World Bank (2023),
μ_{TV}	Natural death rate of tsetse flies	0.03	day^{-1}	Hargrove (2004),
θ_T	Progression rate from exposed to hemolymphatic trypanosomiasis	0.143	day^{-1}	Jamonneau et al. (2012)
α_{HT}	Progression rate from hemolymphatic to meningo-encephalitic stage	0.033	day^{-1}	Kennedy (2013)
γ_{HT}	Treatment rate for hemolymphatic trypanosomiasis	0.1	day^{-1}	Franco et al. (2014)
γ_{MT}	Treatment rate for meningo-encephalitic trypanosomiasis	0.067	day^{-1}	Büscher et al. (2017)
ϑ_T	Recovery rate from trypanosomiasis treatment	0.2	day^{-1}	Priotto et al. (2009)
θ_{TV}	Progression rate from exposed to infected tsetse flies	0.125	day^{-1}	Aksoy et al. (2003)
δ_{HT}	Disease-induced death rate for hemolymphatic trypanosomiasis	0.01	day^{-1}	Odiit, et al. (2004)
δ_{MT}	Disease-induced death rate for meningo-encephalitic trypanosomiasis	0.05	day^{-1}	Blum et al. (2006)
δ_T	Disease-induced death rate for trypanosomiasis treatment class	0.001	day^{-1}	Simarro et al. (2012)
δ_{TV}	Disease-induced death rate for infected tsetse flies	0.02	day^{-1}	Liana et al (2020)

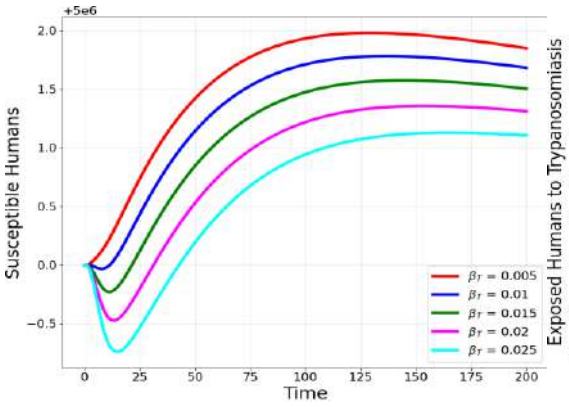

Figure 2: Effect of varying β_T on the susceptible humans

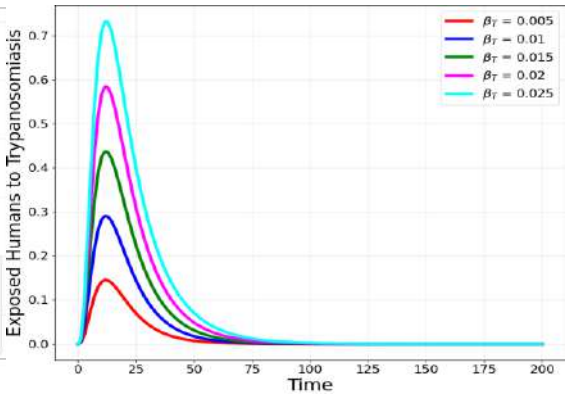

Figure 3: Effect of varying β_T on the exposed humans

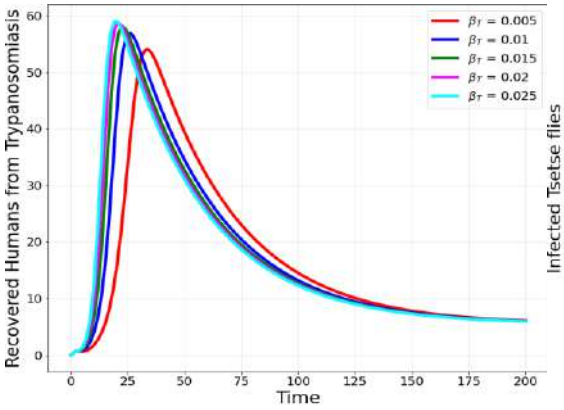

Figure 4: Effect of varying β_T on the recovered humans

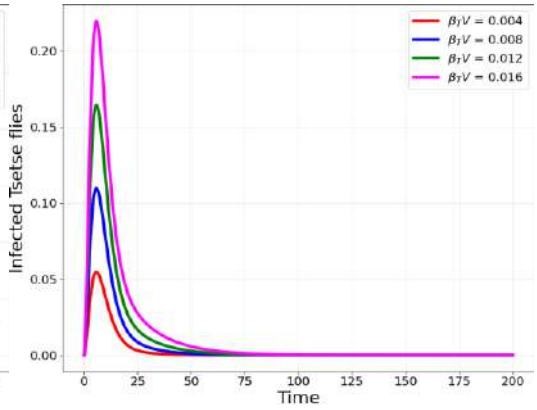

Figure 5: Effect of varying β_T on the infected vectors

Figure **1** displays the temporal evolution of susceptible humans over a 200-day period, showing curved trajectories that initially dip below zero before rising to different equilibrium levels based on varying transmission rates (β_T). The curves exhibit a characteristic dip-and-recovery pattern, with higher β_T values (shown in red and blue) reaching higher final equilibrium states around $1.8-2.0\times10^6$ individuals, while lower transmission rates result in lower equilibria. This pattern reveals that higher transmission rates paradoxically lead to larger susceptible populations at equilibrium because the disease burns through the population more quickly, creating immunity that eventually allows for population recovery. The initial negative dip suggests a mathematical artifact or represents a scenario where disease pressure temporarily overwhelms recruitment, but the system ultimately stabilizes with higher transmission rates supporting larger susceptible populations due to faster cycling through the disease states. Figure **2** illustrates the dynamics of exposed humans to trypanosomiasis, showing sharp peaks that occur early in the epidemic timeline before rapidly declining to near-zero levels. The cyan line ($\beta_T = 0.025$) exhibits the highest and earliest peak around day 20, reaching approximately 0.7 individuals per unit population,

while lower transmission rates show progressively smaller and later peaks. This epidemiological pattern demonstrates that higher transmission rates create more intense but shorter-lived exposure periods, as individuals rapidly progress through the exposed state into active infection. The quick decline to zero indicates that the exposed class is a transient state in the disease progression, with the timing and magnitude of peaks directly correlating with transmission intensity and determining the overall epidemic trajectory.

Figure **3** presents the recovered human population dynamics, characterized by bell-shaped curves that peak around days 30-40 before gradually declining over time. All transmission rate scenarios show similar peak magnitudes (approximately 55-60 individuals), but the curves exhibit different slopes and timing, with higher β_T values creating sharper, earlier peaks followed by steeper declines. This epidemiological significance reflects the temporary nature of immunity in trypanosomiasis, where recovered individuals eventually return to susceptible status through waning immunity (ω_T parameter). The convergence of peak heights across different transmission rates suggests that the total number of individuals who recover is less dependent on transmission intensity than on the overall population dynamics and treatment efficacy, while the declining tails indicate continuous loss of immunity over time. Figure 4 depicts infected vector (tsetse fly) populations using a different parameter set (β_{TV}), showing rapid rise-and-fall dynamics with peaks occurring around days 20-25. The magenta line ($\beta_{TV} = 0.016$) demonstrates the highest peak at approximately 0.23 infected vectors per unit, while all curves rapidly approach zero by day 100. This pattern reflects the vector population's response to human infection levels, where infected vectors proliferate quickly when human cases are abundant but decline rapidly as human infections are controlled through treatment or natural recovery. The epidemiological implication is that vector control timing is critical during the early epidemic phase when vector infection rates peak, and that sustained vector populations require continuous human infection reservoirs to maintain transmission cycles.

5.0 Conclusions

In this research, we formulated a fractional-order mathematical framework to comprehensively examine the transmission dynamics of trypanosomiasis and assess the efficacy of treatment-centered intervention strategies. We employed the Caputo fractional derivative, which enables the model to capture memory effects—a crucial characteristic when investigating vector-borne diseases where the current epidemiological state frequently depends not only on immediate conditions but also on the historical patterns of infection, treatment, and vector-human interactions. Acknowledging the distinctive capacity of fractional models to represent real-world disease transmission patterns with greater fidelity than conventional integer-order systems, we performed a comprehensive theoretical examination of the proposed mathematical framework. Our analysis commenced by establishing the mathematical foundations for solution existence and uniqueness, ensuring the model demonstrates consistent behavior under epidemiologically realistic conditions. To numerically solve the system of fractional differential equations, we implemented the generalized Adams-Bashforth-Moulton predictor-corrector method, a robust computational scheme specifically designed to handle the non-local characteristics inherent in fractional

derivatives. Through extensive computational simulations, we investigated how different values of the fractional order parameter (as characterized by the Caputo operator) and critical epidemiological parameters, including vector biting rates, transmission coefficients, and treatment success rates across different disease stages, influence the temporal evolution of trypanosomiasis transmission within affected populations. The simulation outcomes reveal several epidemiologically significant findings. Notably, increases in vector-human contact rates and transmission probabilities correspond to substantial elevations in disease prevalence across all population compartments. Conversely, enhancing treatment rates and success probabilities for both hemolymphatic and meningo-encephalitic stages significantly reduces infection burdens throughout the community.

Funding

No funding was received for this research.

Credit Authorship Contribution Statement

Musa Yunusa: Writing – original draft, Formal analysis, Methodology. **Omale David:** Writing – review & editing, Validation., **Joseph Egbemhenghe:** Formal analysis, Methodology. **Godwin Onuche Acheneje:** Conceptualization, Writing – review & editing, Formal analysis. **William Atokolo:** Writing – review & editing, Software, Formal analysis.

Declaration of Competing Interest

The authors declare no financial conflicts of interest or personal relationships that could have influenced the work reported in this paper.

Data Availability

All parameter values and initial conditions used in this study are presented in the manuscript tables. The computational code for model simulations is available from the corresponding author upon reasonable request.

References

Abah E., Bolaji B., Atokolo W., Amos J., Acheneje G.O., Omede B.I, Amos J.,Omeje D. (2024), Fractional mathematical model for the Transmission Dynamics and control of Diphtheria ,International Journal of mathematical Analysis and Modelling,Vol.7,ISSN:2682-5694.

Ahmed, E. & El-Sayed, A.M.A. (2007), "Equilibrium points, stability and numerical solutions of fractional-order predator-prey and rabies models," Journal of Mathematical Analysis and Applications, 325(1), pp. 542-553. DOI: 10.1016/j.jmaa.2006.01.087

Aksoy, S., Gibson, W.C. & Lehane, M.J. (2003), "Interactions between tsetse and trypanosomes with implications for the control of trypanosomiasis," Advances in Parasitology, 53, pp. 1-83. DOI: 10.1016/S0065-308X(03)53002-0

Amos J., Omale D., Atokolo W., Abah E., Omede B.I., Acheneje G.O., Bolaji B. (2024), Fractional mathematical model for the Transmission Dynamics and control of Hepatitis C,FUDMA Journal of Sciences,Vol.8,No.5,pp.451-463, DOI: https://doi.org/10.33003/fjs-2024-0805-2883.

Anderson, R.M. & May, R.M. (1991), "Infectious Diseases of Humans: Dynamics and Control," Oxford University Press, Oxford.

Arafa, A.A.M., Rida, S.Z. & Khalil, M. (2012), "Fractional modeling dynamics of HIV and CD4+ T-cells during primary infection," Nonlinear Biomedical Physics, 6(1), pp. 1. DOI: 10.1186/1753-4631-6-1

Atangana, A. & Araz, S.İ. (2020), "Fractional stochastic modelling illustration with modified Chua attractor," European Physical Journal Plus, 135(11), pp. 863. DOI: 10.1140/epjp/s13360-020-00857-w

Atangana, A. & Baleanu, D. (2016), "New fractional derivatives with nonlocal and non-singular kernel: Theory and application to heat transfer model," Thermal Science, 20(2), pp. 763-769. DOI: 10.2298/TSCI160111018A

Atokolo W a, RemigiusAja .O. ,Omale .D., Ahman .Q. O.,Acheneje G. O., Amos.J, Fractional mathematical model for the transmission dynamics and control of Lassa fever Journal of journal homepage: www.elsevier. 2773-1863/© 2024com/locate/fraopehttps:// doi.org/10.1016/j.fraope.2024.100110.

Baleanu, D., Diethelm, K., Scalas, E. & Trujillo, J.J. (2012), "Fractional Calculus: Models and Numerical Methods," World Scientific, Singapore. DOI: 10.1142/8180

Baleanu, D., Jajarmi, A., Mohammadi, H. & Rezapour, S. (2020), "A new study on the mathematical modelling of human liver with Caputo-Fabrizio fractional derivative," Chaos, Solitons & Fractals, 134, pp. 109705. DOI: 10.1016/j.chaos.2020.109705

Blum, J., Schmid, C. & Burri, C. (2006), "Clinical aspects of 2541 patients with second stage human African trypanosomiasis," Acta Tropica, 97(1), pp. 55-64. DOI: 10.1016/j.actatropica.2005.08.001

Büscher, P., Cecchi, G., Jamonneau, V. & Priotto, G. (2017), "Human African trypanosomiasis," Lancet, 390(10110), pp. 2397-2409. DOI: 10.1016/S0140-6736(17)31510-6

Büscher, P., Cecchi, G., Jamonneau, V. & Priotto, G. (2017), "Human African trypanosomiasis," Lancet, 390(10110), pp. 2397-2409. DOI: 10.1016/S0140-6736(17)31510-6

Caputo, M. & Fabrizio, M. (2015), "A new definition of fractional derivative without singular kernel," Progress in Fractional Differentiation and Applications, 1(2), pp. 73-85.

Checchi, F., Funk, S., Chandramohan, D., Haydon, D.T. & Chappuis, F. (2018), "Updated estimate of the duration of the meningo-encephalitic stage in gambiense human African trypanosomiasis," BMC Research Notes, 11(1), pp. 702. DOI: 10.1186/s13104-018-3818-7

Daftardar-Gejji, V. & Jafari, H. (2006), "An iterative method for solving nonlinear functional equations," Journal of Mathematical Analysis and Applications, 316(2), pp. 753-763. DOI: 10.1016/j.jmaa.2005.05.009

Diethelm, K. & Ford, N.J. (2004), "Multi-order fractional differential equations and their numerical solution," Applied Mathematics and Computation, 154(3), pp. 621-640. DOI: 10.1016/S0096-3003(03)00739-2

Diethelm, K. (2010), "The Analysis of Fractional Differential Equations: An Application-Oriented Exposition Using Differential Operators of Caputo Type," Springer-Verlag, Berlin. DOI: 10.1007/978-3-642-14574-2

Diethelm, K., Ford, N.J. & Freed, A.D. (2002), "A predictor-corrector approach for the numerical solution of fractional differential equations," Nonlinear Dynamics, 29(1), pp. 3-22. DOI: 10.1023/A:1016592219341

El-Sayed, A.M.A., El-Mesiry, A.E.M. & El-Saka, H.A.A. (2007), "On the fractional-order logistic equation," Applied Mathematics Letters, 20(7), pp. 817-823. DOI: 10.1016/j.aml.2006.08.013

Franco, J.R., Cecchi, G., Priotto, G., Paone, M., Diarra, A., Grout, L., Mattioli, R.C. & Argaw, D. (2018), "Monitoring the elimination of human African trypanosomiasis: Update to 2016," PLoS Neglected Tropical Diseases, 12(12), pp. e0006890. DOI: 10.1371/journal.pntd.0006890

Franco, J.R., Simarro, P.P., Diarra, A. & Jannin, J.G. (2014), "Epidemiology of human African trypanosomiasis," Clinical Epidemiology, 6, pp. 257-275. DOI: 10.2147/CLEP.S39728

Funk, S., Nishiura, H., Heesterbeek, H., Edmunds, W.J. & Checchi, F. (2013), "Identifying transmission cycles at the human-animal interface: The role of animal reservoirs in maintaining gambiense human African trypanosomiasis," PLoS Computational Biology, 9(1), pp. e1002855. DOI: 10.1371/journal.pcbi.1002855

Garrappa, R. (2018), "Numerical solution of fractional differential equations: A survey and a software tutorial," Mathematics, 6(2), pp. 16. DOI: 10.3390/math6020016

Gervas, E.H., Opoku, A.A., Azangue, N. & Luboobi, L.S. (2018), "Mathematical Modelling of Human African Trypanosomiasis Using Control Measures," Computational and Mathematical Methods in Medicine, 2018, pp. 5293568. DOI: 10.1155/2018/5293568

Hargrove, J.W. (2004), "Tsetse population dynamics," in The Trypanosomiases, I. Maudlin, P.H. Holmes, and M.A. Miles, Eds. Wallingford: CABI Publishing, pp. 113-137. DOI: 10.1079/9780851994758.0113

Hargrove, J.W., Ouifki, R., Kajunguri, D., Vale, G.A. & Torr, S.J. (2012), "Modeling the control of trypanosomiasis using trypanocides or insecticide-treated livestock," PLoS Neglected Tropical Diseases, 6(5), pp. e1615. DOI: 10.1371/journal.pntd.0001615

Hashim, I., Abdulaziz, O. & Momani, S. (2009), "Homotopy analysis method for fractional IVPs," Communications in Nonlinear Science and Numerical Simulation, 14(3), pp. 674-684. DOI: 10.1016/j.cnsns.2007.09.014

Heesterbeek, H., Anderson, R.M., Andreasen, V., Bansal, S., De Angelis, D., Dye, C., Eames, K.T., Edmunds, W.J., Frost, S.D., Funk, S. & Hollingsworth, T.D. (2015), "Modeling infectious disease dynamics in the complex landscape of global health," Science, 347(6227), pp. aaa4339. DOI: 10.1126/science.aaa4339

Jalija, E., Amos, J**.,** Atokolo, W., Omale, D., Abah, E., Alih, U., & **Bolaji, B**. (2025).Numerical investigations on Dengue fever model through singular and non-singular fractional operators. International Journal of Mathematical Analysis and Modelling.

Jalija, E., Amos, J**.,** Atokolo, W., Omale, D., Abah, E., Alih, U., & **Bolaji, B**. (2025).Numerical Solution of fractional order Typhoid Fever and HIV/AIDS co-infection Model Via TheGeneralized Fractional Adams-Bashforth-Moulton Approach. GPH-International Journal of Mathematics, 8(5), 01-31. https://doi.org/10.5281/zenodo.15623363.

Jamonneau, V., Ilboudo, H., Kaboré, J., Kaba, D., Koffi, M., Solano, P., Garcia, A., Courtin, D., Laveissière, C., Lingue, K., Buscher, P. & Bucheton, B. (2012), "Untreated human infections by Trypanosoma brucei gambiense are not 100% fatal," PLoS Neglected Tropical Diseases, 6(6), pp. e1691. DOI: 10.1371/journal.pntd.0001691

Kennedy, P.G.E. (2013), "Clinical features, diagnosis, and treatment of human African trypanosomiasis (sleeping sickness)," Lancet Neurology, 12(2), pp. 186-194. DOI: 10.1016/S1474-4422(12)70296-X

Kennedy, P.G.E. (2019), "Update on human African trypanosomiasis (sleeping sickness)," Journal of Neurology, 266(9), pp. 2334-2337. DOI: 10.1007/s00415-019-09425-7

Khan, M.A., Ullah, S. & Okosun, K.O. (2020), "A fractional order pine wilt disease model with Caputo-Fabrizio derivative," Advances in Difference Equations, 2020(1), pp. 410. DOI: 10.1186/s13662-020-02868-1

Kilbas, A.A., Srivastava, H.M. & Trujillo, J.J. (2006), "Theory and Applications of Fractional Differential Equations," Elsevier, Amsterdam.

Kumar, S., Kumar, A. & Odibat, Z.M. (2017), "A nonlinear fractional model to describe the population dynamics of two interacting species," Mathematical Methods in the Applied Sciences, 40(11), pp. 4134-4148. DOI: 10.1002/mma.4293

Li, Y., Chen, Y. & Podlubny, I. (2010), "Mittag-Leffler stability of fractional order nonlinear dynamic systems," Automatica, 45(8), pp. 1965-1969. DOI: 10.1016/j.automatica.2009.04.003

Liana, M., Wainaina, M., Mayondi, V.G. & Mwangi, J. (2020), "African Trypanosomiasis Dynamics: Modelling the Effects of Treatment, Education, and Vector Trapping," International Journal of Mathematics and Mathematical Sciences, 2020, pp. 3690472. DOI: 10.1155/2020/3690472

Lord, J.S., Hargrove, J.W., Torr, S.J. & Vale, G.A. (2018), "Climate change and African trypanosomiasis vector populations in Zimbabwe's Zambezi Valley: A mathematical modelling study," PLoS Medicine, 15(10), pp. e1002675. DOI: 10.1371/journal.pmed.1002675

Malvy, D. & Chappuis, F. (2011), "Sleeping sickness," Clinical Microbiology and Infection, 17(7), pp. 986-995. DOI: 10.1111/j.1469-0691.2011.03536.x

Mandal, M., Jana, S., Nandi, S.K., Khatua, A., Adak, S. & Kar, T.K. (2021), "A model based study on the dynamics of COVID-19: Prediction and control," Chaos, Solitons & Fractals, 136, pp. 109889. DOI: 10.1016/j.chaos.2020.109889

Momani, S. & Odibat, Z. (2007), "Homotopy perturbation method for nonlinear partial differential equations of fractional order," Physics Letters A, 365(5-6), pp. 345-350. DOI: 10.1016/j.physleta.2007.01.046

Odibat, Z.M. & Shawagfeh, N.T. (2007), "Generalized Taylor's formula," Applied Mathematics and Computation, 186(1), pp. 286-293. DOI: 10.1016/j.amc.2006.07.102

Odiit, M., Bessell, P.R., Fèvre, E.M., Robinson, T., Kinoti, J., Coleman, P.G., Welburn, S.C., McDermott, J. & Woolhouse, M.E.J. (2006), "Using remote sensing and geographic information systems to identify villages at high risk for rhodesiense sleeping sickness in Uganda," Transactions of the Royal Society of Tropical Medicine and Hygiene, 100(4), pp. 354-362. DOI: 10.1016/j.trstmh.2005.04.022

Omede.B. I, Israel. M.,Mustapha .M. K. , Amos J. ,Atokolo .W. , and Oguntolu .F. A. (2024) Approximate solution to the fractional soil transmitted Helminth infection model using Laplace Adomian Decomposition Method.Journal of mathematics. (2024) Int. J. Mathematics. 07(04), 16-40.

Onoja.T.U., Amos J., Atokolo. W., Abah .E. , Omale .D., Acheneje .G. O. & Bolaji B. (2025) Numerical Solution of Fractional order COVID-19 Model Via the Generalized Fractional Adams-Bashforth-Moulton Approach. International Journal of Mathematical Analysis and Modelling.

Pandey, A., Atkins, K.E., Bucheton, B., Camara, M., Aksoy, S., Galvani, A.P. & Funk, S. (2015), "Evaluating long-term effectiveness of sleeping sickness control measures in Guinea," Parasites & Vectors, 8(1), pp. 550. DOI: 10.1186/s13071-015-1121-x

Philip J., Omale D., Atokolo W., Amos J., Acheneje G.O., Bolaji B. (2024), Fractional mathematical model for the Transmission Dynamics and control of HIV/AIDs,FUDMA Journal of Sciences,Vol.8,No.6,pp.451-463, DOI: https://doi.org/10.33003/fjs-2024-0805-2883.

Pinto, C.M.A. & Machado, J.A.T. (2013), "Fractional model for malaria transmission under control strategies," Computers & Mathematics with Applications, 66(5), pp. 908-916. DOI: 10.1016/j.camwa.2012.11.017

Podlubny, I. (1999), "Fractional Differential Equations: An Introduction to Fractional Derivatives, Fractional Differential Equations, to Methods of Their Solution and Some of Their Applications," Academic Press, San Diego.

Priotto, G., Kasparian, S., Mutombo, W., Ngouama, D., Ghorashian, S., Arnold, U., Ghabri, S. & Baudin, E. (2009), "Nifurtimox-eflornithine combination therapy for second-stage African Trypanosoma brucei gambiense trypanosomiasis: A multicentre, randomised, phase III, non-inferiority trial," Lancet, 374(9683), pp. 56-64. DOI: 10.1016/S0140-6736(09)61117-X

Rock, K.S., Stone, C.M., Hastings, I.M., Keeling, M.J., Torr, S.J. & Chitnis, N. (2015), "Mathematical models of human African trypanosomiasis epidemiology," Advances in Parasitology, 87, pp. 53-133. DOI: 10.1016/bs.apar.2014.12.003

Rock, K.S., Torr, S.J., Lumbala, C. & Keeling, M.J. (2017), "Predicting the impact of intervention strategies for sleeping sickness in two high-endemicity health zones of the Democratic Republic of Congo," PLoS Neglected Tropical Diseases, 11(1), pp. e0005162. DOI: 10.1371/journal.pntd.0005162

Simarro, P.P., Cecchi, G., Franco, J.R., Paone, M., Diarra, A., Ruiz-Postigo, J.A., Fèvre, E.M., Mattioli, R.C. & Jannin, J.G. (2012), "Estimating and mapping the population at risk of sleeping sickness," PLoS Neglected Tropical Diseases, 6(10), pp. e1859. DOI: 10.1371/journal.pntd.0001859

Simarro, P.P., Franco, J., Diarra, A., Postigo, J.A.R. & Jannin, J. (2012), "Update on field use of the available drugs for the chemotherapy of human African trypanosomiasis," Parasitology, 139(7), pp. 842-846. DOI: 10.1017/S0031182012000169

Steverding, D. (2008), "The history of African trypanosomiasis," Parasites & Vectors, 1(1), pp. 3. DOI: 10.1186/1756-3305-1-3

Sun, H., Zhang, Y., Baleanu, D., Chen, W. & Chen, Y. (2018), "A new collection of real world applications of fractional calculus in science and engineering," Communications in Nonlinear Science and Numerical Simulation, 64, pp. 213-231. DOI: 10.1016/j.cnsns.2018.04.019

Sweilam, N.H., Khader, M.M. & Al-Bar, R.F. (2007), "Numerical studies for a multi-order fractional differential equation," Physics Letters A, 371(1-2), pp. 26-33. DOI: 10.1016/j.physleta.2007.06.016

World Bank (2023), "Life expectancy at birth, total (years) - Sub-Saharan Africa," World Bank Open Data. Available: https://data.worldbank.org/indicator/SP.DYN.LE00.IN

World Health Organization (2020), "Ending the neglect to attain the Sustainable Development Goals: A road map for neglected tropical diseases 2021–2030," World Health Organization, Geneva.

World Health Organization (2023), "Human African trypanosomiasis (sleeping sickness): Epidemiological update," Weekly Epidemiological Record, 98(10), pp. 95-105.